

A JOINT BIDIAGONALIZATION BASED ALGORITHM FOR LARGE SCALE LINEAR DISCRETE ILL-POSED PROBLEMS IN GENERAL-FORM REGULARIZATION*

ZHONGXIAO JIA[†] AND YANFEI YANG[‡]

Abstract. Based on the joint bidiagonalization process of a large matrix pair $\{A, L\}$, we propose and develop an iterative regularization algorithm for the large scale linear discrete ill-posed problems in general-form regularization: $\min \|Lx\|$ subject to $x \in \mathcal{S} = \{x \mid \|Ax - b\| \leq \tau \|e\|\}$ with a Gaussian white noise e and $\tau > 1$ slightly, where L is a regularization matrix. Our algorithm is different from the hybrid one proposed by Kilmer *et al.*, which is based on the same process but solves the general-form Tikhonov regularization problem: $\min_x \{\|Ax - b\|^2 + \lambda^2 \|Lx\|^2\}$. We prove that the iterates take the form of attractive filtered generalized singular value decomposition (GSVD) expansions, where the filters are given explicitly. This result and the analysis on it show that the method must have the desired semi-convergence property and get insight into the regularizing effects of the method. We use the L-curve criterion or the discrepancy principle to determine k^* . The algorithm is simple and effective, and numerical experiments illustrate that it often computes more accurate regularized solutions than the hybrid one.

Key words. Linear discrete ill-posed, general-form regularization, joint bidiagonalization, GSVD, filtered GSVD expansion, semi-convergence, LSQR, hybrid, discrepancy principle

AMS subject classifications. 65F22, 65F10, 65F35, 65F50, 65J20

1. Introduction. Consider the solution of the large scale linear discrete ill-posed problem

$$(1.1) \quad \min_{x \in \mathbb{R}^n} \|Ax - b\| \quad \text{or} \quad Ax = b, \quad A \in \mathbb{R}^{m \times n}, \quad b \in \mathbb{R}^m,$$

where the norm $\|\cdot\|$ is the 2-norm of a vector, the matrix A is ill conditioned with its singular values decaying to zero with no obvious gap between consecutive ones, and the right-hand side $b = b_{true} + e$ is noisy and assumed to be contaminated by a Gaussian white noise e , where b_{true} is the noise-free right-hand side and $\|e\| < \|b_{true}\|$. Such kind of problem arises in a variety of applications such as computerized tomography, image deblurring, signal processing, geophysics, heat propagation, biomedical and optical imaging, groundwater modeling, and many others; see, e.g., [1, 2, 6, 11, 18, 22, 23]. Since b contains the noise e and A is extremely ill conditioned, the naive solution $x_{naive} = A^\dagger b$ is very large or huge in norm and is a meaningless approximation to the true solution $x_{true} = A^\dagger b_{true}$, where \dagger denotes the Moore-Penrose inverse of a matrix. Therefore, one has to use regularization to obtain a best possible approximation to x_{true} [10, 12].

Assume that $Ax_{true} = b_{true}$ and $m \geq n$. Then two essentially equivalent dominating regularization approaches are the following general-form regularization

$$(1.2) \quad \min \|Lx\| \quad \text{subject to} \quad x \in \mathcal{S} = \{x \mid \|Ax - b\| \leq \tau \|e\|\}$$

with some $\tau > 1$ and the general-form Tikhonov regularization

$$(1.3) \quad \min_x \{\|Ax - b\|^2 + \lambda^2 \|Lx\|^2\},$$

*This work was supported in part by the National Science Foundation of China (No. 11771249).

[†]Department of Mathematical Sciences, Tsinghua University, 100084 Beijing, China (jiazx@tsinghua.edu.cn).

[‡]Department of Mathematical Sciences, Tsinghua University, 100084 Beijing, China (yangyf14@mails.tsinghua.edu.cn).

where $L \in \mathbb{R}^{p \times n}$ is a regularization matrix and $\lambda > 0$ is the regularization parameter. If $L = I_n$, the $n \times n$ identity matrix, then (1.2) and (1.3) are called standard-form regularization problems. If A and L satisfy

$$(1.4) \quad \mathcal{N}(A) \cap \mathcal{N}(L) = \{\mathbf{0}\}, \text{ i.e., } \text{rank} \begin{pmatrix} A \\ L \end{pmatrix} = n,$$

the solution to (1.3) is unique, where $\mathbf{0}$ denotes the zero vector of dimension n . In practical applications, L is typically chosen as a scaled approximation of the first or second derivative operator [10, 12].

For $L \neq I_n$, (1.2) and (1.3) can be transformed to their standard forms with $L = I_n$ and A replaced by AL_A^\dagger , where

$$L_A^\dagger = (I - (A(I - L^\dagger L))^\dagger A) L^\dagger$$

is A -weighted pseudoinverse of L and $L_A^\dagger = L^\dagger$ when $p \geq n$; see [10] for details. This is computationally viable and attractive if not much effort is needed by applying L_A^\dagger , e.g., when L is banded with small bandwidth and has a known null space; we refer the reader to, e.g., [4, 5, 8] for some available algorithms and codes. In many practical applications, however, such transformation is computationally unfeasible. This is often the case for two or three dimensional case, e.g., where L has no special structure or is the sum of Kronecker products such that L_A^\dagger is expensive to use.

There have been some available randomized algorithms and Krylov subspace type methods for solving the regularization problem (1.2) or (1.3) when the application of L_A^\dagger is computationally unfeasible. For example, Jia and Yang [17] have proposed and developed efficient randomized SVD algorithms for solving (1.2) effectively, where a large scale least squares problem is iteratively solved with low or modest accuracy at each step. Several Krylov subspace type methods have been presented to solve (1.3). To shed light on a few existing Krylov subspace type methods, it is important and necessary to keep in mind the basic and core requirements for a regularization method: As far as solving (1.3) is concerned, (i) a good regularized solution must capture the dominant generalized singular value decomposition (GSVD) components of the matrix pair $\{A, L\}$ and meanwhile suppress those corresponding to small generalized singular values, and (ii) the generalized right singular vectors of the matrix pair $\{A, L\}$ form a more suitable basis to express a regularized solution. See [10, 12, 19] for details.

Based on some generalized Arnoldi process proposed first by Li and Ye [21] for the solution of quadratic eigenvalue problems, Reichel *et al.* [28] present a hybrid iterative algorithm for solving (1.3). The generalized Arnoldi process successively reduces the square matrix pair $\{A, L\}$ to a sequence of small matrix pairs $\{H_A, H_L\}$, where the projection matrix H_L quickly becomes full as the number of iterations k increases. The reduction exploits only A and L but does not use their transposes, so the information on A^T and L^T is lacking. This may make the underlying subspace unable to capture a dominant generalized right singular subspace. In fact, for $L = I_n$, Hansen in his book [12, p.126] insightfully summarizes that Arnoldi process based methods, such as RRGMRRES, mix the SVD components in each iteration, their success is highly problem dependent, and they can be successful when the mixing of the SVD components is weak, e.g., A is (nearly) symmetric. It follows from the above that generalized Arnoldi methods have similar limitations. Indeed, we have observed from [28] that the regularized solutions behaved quite irregularly when A is nonsymmetric; see Example 5.1 there. This makes it very hard to stop the algorithm properly.

Hochstenbach *et al.* [13] propose an extended Golub-Kahan bidiagonalization process to reduce the matrix pair $\{A, L\}$ to a sequence of small matrix pairs $\{H_{k+1,k}, K_{k,k}\}$ with $H_{k+1,k}$ and $K_{k,k}$ being upper Hessenberg and triangular, respectively. The process degenerates to the standard Golub-Kahan bidiagonalization process when $L = I_n$. They then develop a hybrid projection algorithm for solving (1.3), which is projected onto a sequence of generalized Krylov subspaces generated by $A^T b$ and the matrices $A^T A$ and $L^T L$ simultaneously. The underlying solution subspace contains the much lower dimensional standard Krylov subspace generated by $A^T b$ and $A^T A$ and that generated by $A^T b$ and $L^T L$ and meanwhile includes too many possibly useless vectors. Precisely, at iteration k , the process produces only $\lfloor \log_2 k \rfloor$ dimensional Krylov subspaces generated by $A^T b$ and $A^T A$ and by $A^T b$ and $L^T L$, respectively, and each iteration computes the matrix-vector products with A^T , A , L^T and L and uses *longer* recurrences during orthonormalization of basis vectors as the iteration *proceeds*; see [13, 30]. In other words, the dimension of generalized Krylov subspace increases *exponentially* when generating a standard Krylov subspace generated by each of $A^T A$ and $L^T L$, respectively. For example, if only fifteen dimensional Krylov subspaces generated by $A^T A$ and $L^T L$ are needed, one has to perform the extended Golub-Kahan bidiagonalization process $2^{15} = 32768$ steps if $2^{15} \leq \min\{n, p\}$, which is very expensive. In the meantime, we should notice that the Krylov subspace generated by $A^T b$ and $A^T A$ favors dominant right singular vectors of the single A , which may bear no relation to those *desired* dominant generalized ones of the matrix pair $\{A, L\}$. In the meantime, it is not yet clear what the whole generalized Krylov subspace favors. We mention that, except Example 4.5 in [13] where it is unclear whether or not A is symmetric, all the other test matrices A in [13, 30] are symmetric, in which case the method is more possible to succeed.

Zha [31] proposes a joint bidiagonalization process that successively reduces the matrix pair $\{A, L\}$ to upper bidiagonal forms. Based on the process, Zha proposes a joint bidiagonalization method for computing a few largest or smallest generalized singular values and the associated singular vectors of a large matrix pair $\{A, L\}$.

Kilmer *et al.* [19] adapt Zha's joint bidiagonalization to discrete linear ill-posed problems in general-form regularization and develop a joint bidiagonalization process that successively reduces the matrix pair $\{A, L\}$ to lower and upper bidiagonal forms. Based on the process, they propose a hybrid projection method for solving (1.3). It is argued in [19] that the underlying solution subspaces are *legitimate* since they appear to be more directly related to the generalized right singular vectors of $\{A, L\}$. Unlike the extended Golub-Kahan bidiagonalization process, the k -step joint bidiagonalization process does not make any possible waste, but at each step it needs the solution of a large scale linear least squares problem with the coefficient matrix $(A^T, L^T)^T$ that is supposed to be solved iteratively, called inner iteration. Therefore, joint bidiagonalization forms an inner-outer iterative process. Fortunately, $(A^T, L^T)^T$ is typically well conditioned as L is typically so in applications [10, 12]. In these cases, the LSQR algorithm [25] can efficiently solve the mentioned least squares problems. At each iteration of the hybrid projection method [19], one solves a small projected general-form Tikhonov regularization problem. Finally, one solves a large scale least squares problem with the coefficient matrix $(A^T, L^T)^T$ to form a regularized solution. The outer iteration proceeds until the regularized solutions stagnate, that is, their accuracy cannot be improved. In the hybrid method, the iteration number do not play the role of the regularization parameter, and one needs to determine an optimal Tikhonov regularization parameter for a projected general-form regularization

problem generated at each outer iteration.

It is well known from, e.g., [10, 12], that any regularization is based on an underlying requirement that the discrete Picard condition for a given problem is satisfied, only under which can one compute a useful regularized solution with some accuracy. Notice that a small projected general-form Tikhonov regularization problem is solved at each outer iteration [19], where one needs to determine an optimal regularization parameter for the small problem itself. This is also the case for any hybrid projection method for solving (1.3). One fundamental fact that is crucial but has received little attention until the work [9, 27] is: With $L = I_n$, that (1.3) satisfies the discrete Picard condition does not mean that the projected problems fulfill discrete Picard conditions too, and known sufficient conditions for the projected problems to satisfy the discrete Picard conditions require that the singular values of the matrices involved in the projected problems approximate the large singular values of A in natural order. An adaption of this result to $L \neq I_n$ says that the projected problems are guaranteed to inherit the discrete Picard conditions when the generalized singular values of the projected matrix pairs approximate the large generalized singular values of the matrix pair $\{A, L\}$ in natural order. However, it has been proved in [14, 15] that, for $L = I_n$ and LSQR, the approximations in natural order can be guaranteed only for severely ill-posed problems and some moderately ill-posed ones and such property generally does not hold when the singular values of A or the generalized ones of $\{A, L\}$ decay slowly, e.g., those matrices in mildly ill-posed problems. For the definition of severely, moderately and mildly ill-posed problems, see [10, 12].

If the above sufficient conditions are met, the iterative algorithm used resembles the truncated GSVD (TGSVD) method [10] until the occurrence of semi-convergence. At this time, a best regularized solution has been already found and is as accurate as the best TGSVD solution, which is a best regularized solution of (1.1) in the sense of the regularization formulation (1.2). Therefore, one only needs to determine the semi-convergence point by some parameter-choice methods, e.g., the L-curve criterion and the discrepancy principle. We should be aware that, for a hybrid iterative method, whenever the discrete Picard conditions for the projected problems fail to satisfy or are satisfied poorly, i.e., their solution norms (very) large, optimal regularization parameters for them are poorly defined. In this case, a direct consequence is that the regularized solutions may exhibit irregular behavior. When developing a hybrid LSQR variant, by requiring that the singular values of the projected matrices approximate the large singular values of A in natural order, Renaut *et al.* [27] prove that an optimal regularization parameter for each projected problem can be reliably determined by a weighted generalized cross-validation (WGCV) parameter-choice method and it converges to the global optimal regularization parameter λ_{opt} for (1.3) as outer iterations proceed, so that the regularized solutions ultimately stagnate.

In this paper, based on joint bidiagonalization process [19], instead of developing any hybrid projection based algorithm, we will propose a pure projection iterative algorithm for solving (1.2) other than the equivalent (1.3) as done in [19]. Our algorithm is much simpler than the hybrid one [19], and the iteration number k plays the role of the regularization parameter. First, we make use of the joint bidiagonalization process to project (1.2) onto a sequence of low dimensional subspaces and obtain a sequence of projected problems, which involve matrix pairs of small size. Then at each outer iteration we solve a projected problem. Remarkably, we find out that the solution of each of them reduces to an *ordinary* small least squares problem with the coefficient matrix being single lower bidiagonal other than the matrix pair, so that it

is very cheap and reliable to solve it by the QR factorization at $\mathcal{O}(k)$ flops. Another big benefit is that we no longer determine the optimal regularization parameter for each projected problem, which itself may be poorly defined. We make a theoretical analysis on the proposed method and establish a number of results. Most importantly, we first prove that the iterates obtained by our algorithm take the form of filtered GSVD expansions and are expressed *explicitly* in the generalized right singular vector basis of $\{A, L\}$, a desired and insightful property. Then we analyze the filters in the expansions, shed light on the regularizing effects of the algorithm, and prove that the iterates capture dominant GSVD components of $\{A, L\}$, as desired. The results indicate that our algorithm must have the typical semi-convergence property: As the joint bidiagonalization process proceeds, more and more dominant generalized singular components of $\{A, L\}$ are captured, and the regularized solutions converge to the true solution x_{true} of (1.1) until some iteration, after which the regularized solutions start to be deteriorated by the noise e and instead converge to x_{naive} .

As it will turn out, since the residual norms monotonically decrease and the semi-norms of solutions practically increase monotonically, we can use the L-curve criterion and the discrepancy principle to estimate the optimal regularization parameter k^* , at which the semi-convergence occurs.

We will numerically compare our algorithm with the hybrid algorithm in [19], in which we make use of the GCV and WGCV parameter choice methods to determine an optimal regularization parameter for each small projected problem. We are primarily concerned with the accuracy of the best regularized solutions by our algorithm and the hybrid one. The experiments on several real-world problems will illustrate the superiority of our algorithm.

The paper is organized as follows. In Section 2, we overview GSVD, the general-form Tikhonov regularization method and the TGSVD method, and present the joint bidiagonalization process of $\{A, L\}$. In Section 3, we describe the hybrid method in [19]. In Section 4, we propose our joint bidiagonalization based method for solving (1.2). In Section 5, we make a theoretical analysis on it. In Section 6, we consider the practical determination of the optimal regularization parameter. Numerical experiments are presented in Section 7. Finally, we conclude the paper in Section 8.

2. GSVD, regularization methods and joint bidiagonalization. In this section, we provide some necessary background. We describe GSVD, the TGSVD method, the filtered GSVD method, and the joint bidiagonalization process proposed in [31] and developed in [19].

Consider the compact QR factorization

$$(2.1) \quad \begin{pmatrix} A \\ L \end{pmatrix} = QR,$$

where $Q = \begin{pmatrix} Q_A \\ Q_L \end{pmatrix} \in \mathbb{R}^{(m+p) \times n}$ is column orthonormal with $Q_A \in \mathbb{R}^{m \times n}$, $Q_L \in \mathbb{R}^{p \times n}$, and $R \in \mathbb{R}^{n \times n}$ is upper triangular and nonsingular because of the assumption (1.4). We have $A = Q_A R$, $L = Q_L R$, and $Q_A^T Q_A + Q_L^T Q_L = I_n$.

Let the CS decomposition of the matrix pair $\{Q_A, Q_L\}$ be

$$(2.2) \quad Q_A = P_A C W^T, \quad Q_L = P_L S W^T,$$

where $P_A \in \mathbb{R}^{m \times m}$, $P_L \in \mathbb{R}^{p \times p}$, and $W \in \mathbb{R}^{n \times n}$ are orthogonal, and $C \in \mathbb{R}^{m \times n}$ and $S \in \mathbb{R}^{p \times n}$ are diagonal matrices satisfying $C^T C + S^T S = I_n$; see [3, Section 4.2].

Then the GSVD of $\{A, L\}$ is

$$(2.3) \quad A = P_A C G^{-1}, \quad L = P_L S G^{-1}$$

with $G = (g_1, g_2, \dots, g_n) = R^{-1}W \in \mathbb{R}^{n \times n}$, and the vectors g_i are the generalized right singular vectors of $\{A, L\}$. Following the unconventional but more convenient way [19], we order the entries of the diagonal matrices C and S so that

$$(2.4) \quad 1 \geq c_1 \geq \dots \geq c_{\min\{n,p\}} \geq 0, c_{\min\{n,p\}+1} = \dots = c_n = 1,$$

$$(2.5) \quad 0 \leq s_1 \leq \dots \leq s_{\min\{n,p\}} \leq 1.$$

By the GSVD (2.3), the general-form Tikhonov solution x_λ to (1.3) takes a filtered GSVD expansion:

$$(2.6) \quad \begin{aligned} x_\lambda &= (A^T A + \lambda^2 L^T L)^{-1} A^T b = G(C^T C + \lambda^2 S^T S)^{-1} C^T P_A^T b \\ &= \sum_{i=1}^{\min\{n,p\}} \frac{c_i^2}{c_i^2 + \lambda^2 s_i^2} \frac{p_{i,A}^T b}{c_i} g_i + \sum_{i=\min\{n,p\}+1}^n p_{i,A}^T b g_i, \end{aligned}$$

where $P_A = (p_{1,A}, p_{2,A}, \dots, p_{m,A})$, $f_i = \frac{c_i^2}{c_i^2 + \lambda^2 s_i^2}$ are filters, and the second term lies in the null space $\mathcal{N}(L)$ of L , which is spanned by the vectors $g_{\min\{n,p\}+1}, \dots, g_n$. We address that the regularization does not affect the second term. This is simply the filtered GSVD method for solving (1.3).

The discrete Picard condition [10] states that the Fourier coefficients $|p_{i,A}^T b|$ must, on average, decay faster than the c_i . Hence the $|p_{i,A}^T b|$ decay until the Gaussian white noise e dominates the $|p_{i,A}^T b|$, that is, the $|p_{i,A}^T b| \approx |p_{i,A}^T e|$ stagnates and is dominated by e after $i > k_0$ for some k_0 , while $|p_{i,A}^T b| \approx |p_{i,A}^T b_{true}|$ is dominated by b_{true} , $i = 1, 2, \dots, k_0$, where k_0 is called the transition or cutting-off point. Therefore, a good regularized solution x_λ must capture the k_0 dominant GSVD components of $\{A, L\}$ and meanwhile dampen those for $i > k_0$ as much as possible. An optimal regularization parameter λ_{opt} can be determined by some parameter-choice methods, e.g., the discrepancy principle, the L-curve criterion, and the generalized cross validation (GCV) or weighted GCV (WGCV) method; see [10, 12] and also [2, 11].

Alternatively, making use of the GSVD of $\{A, L\}$, one can develop the TGSVD method and computes a sequence of the TGSVD solutions

$$(2.7) \quad x_k^{tgsvd} = \sum_{i=1}^k \frac{p_{i,A}^T b}{c_i} g_i + \sum_{i=\min\{n,p\}+1}^n p_{i,A}^T b g_i, \quad k = 1, 2, \dots, \min\{n, p\},$$

where the first term consists of the first k dominant GSVD components of $\{A, L\}$. The TGSVD solution takes a special filtered GSVD expansion, where the filters $f_i = 1$ for $i = 1, 2, \dots, k$ and $f_i = 0$ for $i = k+1, \dots, \min\{n, p\}$. Under the discrete Picard condition, the TGSVD method exhibits semi-convergence: x_k^{tgsvd} and Lx_k^{tgsvd} converge to x_{true} and Lx_{true} for $k \leq k_0$, afterwards they diverge and instead converge to x_{naive} and Lx_{naive} , respectively. A best possible TGSVD solution $x_{k_0}^{tgsvd}$ is thus obtained for $k = k_0$.

We notice that the second terms in (2.6) and (2.7) are the same and they disappear when $p \geq n$. For later use, we write them as

$$(2.8) \quad g_{\perp} = \sum_{i=\min\{n,p\}+1}^n p_{i,A}^T b g_i \in \mathcal{N}(L).$$

Now we review a procedure that jointly diagonalizes the matrix pair $\{A, L\}$ to lower and upper bidiagonal forms. Applying the BIDIAG-1 algorithm and BIDIAG-2 algorithm in [25] to Q_A and Q_L , respectively, which are the lower and upper Lanczos bidiagonalization processes, we can reduce Q_A and Q_L to lower and upper bidiagonal forms, respectively. The two processes can be written in matrix form:

$$(2.9) \quad Q_A V_k = U_{k+1} B_k, \quad Q_A^T U_{k+1} = V_k B_k^T + \alpha_{k+1} v_{k+1} e_{k+1}^T,$$

$$(2.10) \quad Q_L \hat{V}_k = \hat{U}_k \hat{B}_k, \quad Q_L^T \hat{U}_k = \hat{V}_k \hat{B}_k^T + \hat{\beta}_k \hat{v}_{k+1} e_k^T,$$

where e_{k+1} and e_k are the $(k+1)$ th and k th canonical vectors of dimensions $k+1$ and k , respectively,

$$(2.11) \quad U_{k+1} = (u_1, \dots, u_{k+1}) \in \mathbb{R}^{m \times (k+1)}, \quad \hat{U}_k = (\hat{u}_1, \dots, \hat{u}_k) \in \mathbb{R}^{p \times k},$$

and

$$(2.12) \quad V_k = (v_1, \dots, v_k) \in \mathbb{R}^{n \times k}, \quad \hat{V}_k = (\hat{v}_1, \dots, \hat{v}_k) \in \mathbb{R}^{n \times k}$$

are column orthonormal, and

$$(2.13) \quad B_k = \begin{pmatrix} \alpha_1 & & & & \\ \beta_2 & \alpha_2 & & & \\ & \beta_3 & \ddots & & \\ & & \ddots & \alpha_k & \\ & & & \beta_{k+1} & \end{pmatrix} \in \mathbb{R}^{(k+1) \times k}, \quad \hat{B}_k = \begin{pmatrix} \hat{\alpha}_1 & \hat{\beta}_1 & & & \\ & \hat{\alpha}_2 & \ddots & & \\ & & \ddots & \hat{\beta}_{k-1} & \\ & & & \hat{\alpha}_k & \end{pmatrix} \in \mathbb{R}^{k \times k}$$

are lower bidiagonal and upper bidiagonal, respectively. Zha [31] and Kilmer *et al.* [19] have investigated the relationships between V_k and \hat{V}_k defined in (2.12) and between B_k and \hat{B}_k defined in (2.13), respectively, and they have established the following result.

THEOREM 2.1. *If $v_1 = \hat{v}_1$ in (2.12), then*

$$(2.14) \quad \hat{v}_{j+1} = (-1)^j v_{j+1}, \quad \hat{\alpha}_j \hat{\beta}_j = \alpha_{j+1} \beta_{j+1}, \quad j = 1, \dots, k.$$

A combination of (2.9)–(2.13), Theorem 2.1 and the QR factorization (2.1) shows that A and L can be jointly bidiagonalized [19, 31], as summarized below.

THEOREM 2.2. *Assume that $A \in \mathbb{R}^{m \times n}$ and $L \in \mathbb{R}^{p \times n}$ with $m \geq n$. Then there exist orthogonal matrices $U \in \mathbb{R}^{m \times m}$, $\hat{U} \in \mathbb{R}^{p \times p}$ and $V \in \mathbb{R}^{n \times n}$, and a lower bidiagonal $B \in \mathbb{R}^{m \times n}$, an upper bidiagonal $\bar{B} \in \mathbb{R}^{p \times n}$, and an invertible Z such that*

$$(2.15) \quad A = UBZ^{-1},$$

$$(2.16) \quad L = \hat{U}\bar{B}Z^{-1},$$

where $Z = R^{-1}V$ and $\bar{B} = \hat{B}D$ with $D = \text{diag}(1, -1, 1, -1, \dots)$, and the remaining matrices are obtained by running joint bidiagonalization to completion. In particular, when $p < n$, the columns $p+1, \dots, n$ of \bar{B} contain only zero entries.

From (2.15) and (2.16), we obtain k -step joint bidiagonalization relations

$$(2.17) \quad AZ_k = U_{k+1}B_k,$$

$$(2.18) \quad LZ_k = \hat{U}_k\bar{B}_k,$$

where $Z_k \in \mathbb{R}^{n \times k}$ is the first k columns of Z , and B_k and \bar{B}_k are the first $(k+1) \times k$ and $k \times k$ submatrices of B and \bar{B} , respectively.

For A and L large, the QR factorization (2.1) is impractical. In order to avoid explicitly computing Q_A and Q_L , inspired by Zha's work [31], Kilmer *et al.* [19] develop a joint bidiagonalization (JBD) process, denoted by Algorithm 1, to compute the matrices in (2.11)–(2.13), in which 0_p denotes the zero vector of dimension p .

Algorithm 1 k -step joint bidiagonalization (JBD) process.

- 1: $\beta_1 u_1 = b, \beta_1 = \|b\|.$
 - 2: $\alpha_1 \tilde{v}_1 = QQ^T \begin{pmatrix} u_1 \\ 0_p \end{pmatrix}.$
 - 3: $\hat{\alpha}_1 \hat{u}_1 = \tilde{v}_1(m+1 : m+p)$
 - 4: **for** $i = 1, 2, \dots, k$ **do**
 - 5: $\beta_{i+1} u_{i+1} = \tilde{v}_i(1 : m) - \alpha_i u_i.$
 - 6: $\alpha_{i+1} \tilde{v}_{i+1} = QQ^T \begin{pmatrix} u_{i+1} \\ 0_p \end{pmatrix} - \beta_{i+1} \tilde{v}_i.$
 - 7: $\hat{\beta}_i = (\alpha_{i+1} \beta_{i+1}) / \hat{\alpha}_i.$
 - 8: $\hat{\alpha}_{i+1} \hat{u}_{i+1} = (-1)^i \tilde{v}_{i+1}(m+1 : m+p) - \hat{\beta}_i \hat{u}_i.$
 - 9: **end for**
-

Let $\tilde{u}_i = \begin{pmatrix} u_i \\ 0_p \end{pmatrix}$. At each iteration $i = 1, 2, \dots, k+1$, Algorithm 1 needs to compute $QQ^T \tilde{u}_i$, which is not accessible since Q is not available. However, notice that $QQ^T \tilde{u}_i$ is nothing but the orthogonal projection of \tilde{u}_i onto the column space of $\begin{pmatrix} A \\ L \end{pmatrix}$, which means that $QQ^T \tilde{u}_i = \begin{pmatrix} A \\ L \end{pmatrix} \tilde{x}_i$. Clearly, \tilde{x}_i is the solution to the least squares problem:

$$(2.19) \quad \tilde{x}_i = \arg \min_{\tilde{x} \in \mathbb{R}^n} \left\| \begin{pmatrix} A \\ L \end{pmatrix} \tilde{x} - \tilde{u}_i \right\|.$$

Since the least squares problem is large scale, it is generally only feasible to solve it by an iterative solver, e.g., the most commonly used LSQR algorithm [25]. Here we have two remarks.

REMARK 2.1. *Theoretically, at outer iteration k , the inner least square problem (2.19) is solved accurately in order to guarantee that (2.17) and (2.18) hold exactly. It is unknown whether or not the solution accuracy can be relaxed by allowing possibly large inexactness in the algorithm [19] and ours to be presented later. This issue is certainly complicated. We do not investigate it in the current paper. In finite precision arithmetic, we suppose that (2.19) is solved by the Matlab function `lsqr.m` with the default stopping criterion 10^{-6} .*

REMARK 2.2. *To ensure the numerical orthogonality of the computed U_{k+1} , \hat{U}_k and V_k , we use one step reorthogonalization during the process in implementations.*

3. The hybrid projection based method in [19].

Algorithm 1 takes

$$(3.1) \quad U_{k+1}(\beta_1 e_1) = b, \quad \beta_1 = \|b\|,$$

where e_1 is the first canonical vector of dimension $k+1$. For a given regularization parameter λ , the hybrid projection based method in [19] seeks the solution $x_k^\lambda \in \text{span}\{Z_k\}$ such that

$$\min_{x \in \text{span}\{Z_k\}} \{\|Ax - b\|^2 + \lambda^2 \|Lx\|^2\} = \|Ax_k^\lambda - b\|^2 + \lambda^2 \|Lx_k^\lambda\|^2.$$

Exploit (3.1), (2.17) and (2.18), and write

$$(3.2) \quad x_k^\lambda = Z_k y_k^\lambda.$$

It is direct to justify that

$$\begin{aligned} \|Ax_k^\lambda - b\|^2 + \lambda^2 \|Lx_k^\lambda\|^2 &= \|B_k y_k^\lambda - \beta_1 e_1\|^2 + \lambda^2 \|\bar{B}_k y_k^\lambda\|^2 \\ &= \min_y \{\|B_k y - \beta_1 e_1\|^2 + \lambda^2 \|\bar{B}_k y\|^2\}. \end{aligned}$$

Therefore, at iteration k the hybrid projection based method in [19] solves a projected general-form Tikhonov regularization problem

$$(3.3) \quad \min_y \{\|B_k y - \beta_1 e_1\|^2 + \mu_k^2 \|\bar{B}_k y\|^2\},$$

where the new notation $\mu_k > 0$ is introduced to specialize the regularization parameter for the projected problem at iteration k . The key is the determination of an optimal regularization μ_{kopt} for (3.3). Following the results of Renaut *et al.* [27] with $L = I_n$ to (3.3), the optimal μ_{kopt} determined by the GCV or WGCV method converges to the global optimal regularization parameter λ_{opt} for (1.3) as k increases under the assumption that the generalized singular values of $\{B_k, \bar{B}_k\}$ approximate the large singular values of $\{A, L\}$ in natural order; if the assumption is not fulfilled, such convergence may fail, implying that the regularized solution $x_k^{\mu_{kopt}}$ may behave irregularly and does not stabilize for k sufficiently large. As a consequence, it may be hard to stop the hybrid algorithm properly, and even for k sufficiently large the regularized solution $x_k^{\mu_{kopt}}$ may not be as accurate as $x_{\lambda_{opt}}$, the best regularized solution to (1.3) associated with $\lambda = \lambda_{opt}$.

Now we show how to compute x_k^λ when y_k^λ is known. Let $\tilde{V}_k = (\tilde{v}_1, \dots, \tilde{v}_k) \in \mathbb{R}^{(m+p) \times k}$ be generated by Algorithm 1. Then

$$(3.4) \quad \tilde{V}_k = QV_k = QR(R^{-1}V_k) = \begin{pmatrix} A \\ L \end{pmatrix} Z_k,$$

from which, (2.1) and (3.2) it follows that

$$(3.5) \quad \begin{pmatrix} A \\ L \end{pmatrix} x_k^\lambda = \tilde{V}_k y_k^\lambda.$$

Kilmer *et al.* [19] show that one only needs to form x_k^λ explicitly when it is accepted as the final regularized solution.

Regarding the determination of λ_{opt} , other than determining μ_{kopt} for each projected problem (3.3), Kilmer *et al.* [19] use the L-curve criterion to tentatively estimate

λ_{opt} . They assume that a set of λ -values is prescribed, and derive some update formulas for all the quantities, including regularized solutions, residual norms, and the semi-norms $\|Lx_k^\lambda\|$, which can be efficiently computed for the a-prior set of λ -values. For sufficiently large k at which all the needed dominant GSVD components of $\{A, L\}$ are thought to have been captured, drawing the picture of $(\log \|Ax_k^\lambda - b\|, \log \|Lx_k^\lambda\|)$ for the given set of λ -values, they attempt to obtain a L-curve and pick up the λ -value at the corner as an approximation λ_{opt} .

Their approach to determining λ_{opt} faces two challenging issues: The first is how to effectively determine a sufficiently large k , and the second is how to choose a good a-prior set of λ -values which include the optimal regularization parameter λ_{opt} or its good approximation. As a matter of fact, the first issue is common in any hybrid LSQR algorithm, and there has been no reliable approach to determine it. In our implementation, we will take a regular manner, as done in, e.g., [10, 27], and determine μ_{kopt} for each (3.3) by the GCV code [11] and the WGCV code adapted from [2], both of which need to compute the GSVD of $\{B_k, \bar{B}_k\}$ at cost of $\mathcal{O}(k^3)$ flops.

4. Our joint bidiagonalization based algorithm. Instead of solving (1.3), we now present a joint bidiagonalization based algorithm for solving (1.2), which is a purely iterative regularization method *without* explicitly regularizing projected problems at each outer iteration. In the algorithm, the iteration number k plays the role of the regularization parameter. We will establish a number of important results, which get insight into the regularizing effects of the proposed method and particularly prove that the method has the desired semi-convergence.

Still, we seek $x_k \in \text{span}\{Z_k\}$ and write it in the form

$$(4.1) \quad x_k = Z_k y_k.$$

We aim to project the original large scale regularization problem (1.2) onto a sequence of low dimensional subspaces $\text{span}\{Z_k\}$ and compute regularized solutions x_k from them. We will consider when to terminate and how to practically determine a best regularized solution in Section 6.

From (4.1), the above projection is equivalent to replacing A and L by AZ_k and LZ_k in (1.2) and solving the *reduced* general-form regularization problem

$$(4.2) \quad \min \|LZ_k y\| \quad \text{subject to} \quad y \in \{y \mid \|AZ_k y - b\| = \min\}$$

for y_k , starting with $k = 1$ onwards. Make use of (3.1), (2.17) and (2.18). Then (4.2) becomes the *reduced* general-form regularization problem

$$(4.3) \quad \min \|\bar{B}_k y\| \quad \text{subject to} \quad y \in \{y \mid \|B_k y - \beta_1 e_1\| = \min\}$$

starting with $k = 1$ onwards. After the solution y_k for (4.3) is computed, in terms of (3.4), (2.1) and $x_k = Z_k y_k$, we then compute x_k by solving

$$(4.4) \quad \begin{pmatrix} A \\ L \end{pmatrix} x_k = \tilde{V}_k y_k.$$

Now let us investigate the solution of the constrained problem (4.3). As it will turn out, (4.3) amounts to an ordinary unconstrained linear least squares problem, as shown below.

THEOREM 4.1. *Assume that Algorithm 1 does not break down at iteration $k \leq \min\{n, p\}$. Then the solution y_k to (4.3) is*

$$(4.5) \quad y_k = \arg \min_{y \in \mathbb{R}^k} \|B_k y - \beta_1 e_1\| = \beta_1 B_k^\dagger e_1.$$

Proof. Let $\tilde{y} = \bar{B}_k y$. Then under the assumption on Algorithm 1, \bar{B}_k is nonsingular. Therefore, (4.3) is equivalent to

$$\min \|\tilde{y}\| \quad \text{subject to} \quad \tilde{y} \in \{\tilde{y} \mid \|(B_k \bar{B}_k^{-1})\tilde{y} - \beta_1 e_1\| = \min\}.$$

Notice that B_k is of column full rank, so is $B_k \bar{B}_k^{-1}$. As a result, we have

$$\begin{aligned} \tilde{y}_k &= \beta_1 (B_k \bar{B}_k^{-1})^\dagger e_1 \\ &= \beta_1 (\bar{B}_k B_k^\dagger) e_1 \end{aligned}$$

with the second relation holding because B_k is of column full rank and \bar{B}_k is nonsingular. Then the solution y_k to (4.3) is

$$y_k = \bar{B}_k^{-1} \tilde{y}_k = \beta_1 \bar{B}_k^{-1} ((\bar{B}_k B_k^\dagger) e_1) = \beta_1 B_k^\dagger e_1. \quad \square$$

(4.5) indicates that y_k is simply the solution to the ordinary least squares problem $\min_y \|B_k y - \beta_1 e_1\|$ and \bar{B}_k is not invoked. Let

$$(4.6) \quad B_k = Q_k R_k$$

be the compact QR factorization of B_k , which can be computed by exploiting Givens rotations at cost of $\mathcal{O}(k)$ flops. From (4.5), we obtain

$$(4.7) \quad y_k = \beta_1 R_k^{-1} Q_k^T e_1$$

at cost of $\mathcal{O}(k)$ flops; see [25] for details.

Next, we consider the efficient computation of the residual norm $\|Ax_k - b\|$ and the semi-norm $\|Lx_k\|$.

THEOREM 4.2. *Let the matrices U_{k+1} , \hat{U}_k , B_k and \bar{B}_k be defined in (2.17) and (2.18). Then*

$$(4.8) \quad \|Ax_k - b\| = \|B_k y_k - \beta_1 e_1\|,$$

$$(4.9) \quad \|Lx_k\| = \|\bar{B}_k y_k\|.$$

Proof. Notice $x_k = Z_k y_k$, and exploit (3.1) and (2.17). We obtain

$$Ax_k = AZ_k y_k = U_{k+1} B_k y_k.$$

Since U_{k+1} is column orthonormal, it is direct to derive (4.8) by the orthogonal invariance of the 2-norm. Similarly, we have

$$(4.10) \quad Lx_k = LZ_k y_k = \hat{U}_k \bar{B}_k y_k.$$

Since \hat{U}_k is column orthogonormal, we have (4.9). \square

This theorem shows that, by making use of structures of B_k and \bar{B}_k , both $\|Ax_k - b\|$ and $\|Lx_k\|$ can be computed very efficiently at cost of $\mathcal{O}(k)$ flops without forming x_k explicitly. We only need to compute x_k by solving (4.4) when x_k is accepted as the best regularized solution.

5. Regularization properties of the joint bidiagonalization based algorithm. Now we analyze our algorithm, establish some important results, and get insight into its regularizing effects. Let $\tilde{w} = Rx$. Then by (2.1), we have

$$(5.1) \quad \min_x \|Ax - b\| = \min_{\tilde{w}} \|Q_A \tilde{w} - b\|.$$

First, it is direct to establish the following result, similar to Theorem 4.3 and (3.4) in [19].

LEMMA 5.1. *Let x_k be the regularized solution obtained by our algorithm. Then*

$$(5.2) \quad x_k = R^{-1} \tilde{w}_k, \quad \tilde{w}_k = \arg \min_{\tilde{w} \in \mathcal{K}_k} \|Q_A \tilde{w} - b\|,$$

where \mathcal{K}_k is the k dimensional Krylov subspace

$$(5.3) \quad \mathcal{K}_k = \text{span}\{Q_A^T b, (Q_A^T Q_A) Q_A^T b, \dots, (Q_A^T Q_A)^{k-1} Q_A^T b\},$$

and the solution subspace

$$(5.4) \quad \text{span}\{Z_k\} = R^{-1} \mathcal{K}_k = \text{span}\{G(C^T C)^i C^T P_A^T b\}_{i=0}^{k-1},$$

the k -dimensional Krylov subspace generated by the starting vector $GC^T P_A^T b$ and the matrix $C^T C$, where C is defined by (2.2).

Proof. Write $\tilde{w} = V_k y$, where V_k is generated by (2.9) and $\text{span}\{V_k\} = \mathcal{K}_k$. Then from (2.9) we obtain

$$\min_{\tilde{w} \in \mathcal{K}_k} \|Q_A \tilde{w} - b\| = \min_y \|B_k y - \beta_1 e_1\|.$$

Let $y_k = \arg \min_y \|B_k y - \beta_1 e_1\|$. By the definition (3.4) of Z_k , we have $x_k = Z_k y_k = R^{-1} V_k y_k = R^{-1} \tilde{w}_k$. A direct justification using (2.2) and (2.3) shows (5.4). \square

To present our main theoretical result and make an insightful analysis on the regularizing effects of the proposed algorithm, we need to make some necessary preparations and notation changes. Firstly, for the regularization matrix $L \in \mathbb{R}^{p \times n}$ of rank $\min\{n, p\}$, from the SVD (2.2) of Q_A and Q_L and the labeling orders (2.4) and (2.5), it is obvious that the singular values c_i and s_i must satisfy

$$0 < c_i, \quad s_i < 1, \quad i = 1, 2, \dots, \min\{n, p\}.$$

If $p \geq n$, we retain the notation (2.2) and (2.4), and have $1 > c_1 \geq c_2 \geq \dots \geq c_n > 0$. If $p < n$, different from (2.4), we relabel the c_i and use the new notation

$$(5.5) \quad 1 = c_1 > c_2 \geq c_3 \geq \dots \geq c_{p+1},$$

where $c_1 = 1$ is the largest singular value of Q_A with the multiplicity $n - p$. That is, we reassign the indices i of c_i defined by (2.4) to $i + 1$, $i = 1, 2, \dots, p$, and shift the largest singular value of Q_A to $c_1 = 1$ with multiplicity $n - p$ in (2.4). Correspondingly, we permute the columns of P_A and W in Q_A defined by (2.2), and G defined by (2.3) by moving their respective last $n - p$ columns to the first ones and renaming

$$\begin{aligned} P_A &:= (P_{1,A}, p_{2,A}, \dots, p_{m-n+p+1,A}), \\ W &:= (W_1, w_2, \dots, w_{p+1}), \\ G &:= (G_1, g_2, \dots, g_{p+1}). \end{aligned}$$

With the new notation, we have the range $\mathcal{R}(G_1) = \mathcal{N}(L)$, i.e., $LG_1 = 0$. Keep in mind that if $p \geq n$ then P_A , W and G remain the same as in (2.2) and (2.3), and $\mathcal{N}(L) = \{\mathbf{0}\}$.

Secondly, it is well known [3] that the Lanczos bidiagonalization method for computing the singular values c_i of Q_A with the starting vector $b/\|b\|$ mathematically amounts to the symmetric Lanczos method for computing the eigenvalues c_i^2 of $Q_A^T Q_A$ with the starting vector $Q_A^T b/\|Q_A^T b\|$. It is remarkable that the symmetric Lanczos method works on $Q_A^T Q_A$ as if $Q_A^T Q_A$ has only simple eigenvalues c_i^2 [26]. As a consequence, the Lanczos bidiagonalization method works on Q_A as if the singular values c_i of Q_A are all simple. Notice that the singular values \tilde{c}_i , called the Ritz values, of the projected matrix B_k are always simple provided that the Lanczos bidiagonalization process does not break down at step k . The Lanczos bidiagonalization method uses the \tilde{c}_i as approximations to the k distinct singular values c_i of Q_A . For a rigorous and complete derivation and many details, we refer to [16].

Next we establish an attractive and desired property that the regularized solution x_k has a filtered GSVD expansion and is *explicitly* expressed in the generalized right singular vector basis $\{g_i\}_{i=1}^n$ of $\{A, L\}$.

THEOREM 5.2. *Assume that the c_i are labeled as (5.5) and simple for $p < n$, the matrices P_A , W and G defined as above, and g_\perp defined by (2.8). Then*

$$(5.6) \quad x_k = f_1^{(k)} g_\perp + \sum_{i=2}^{p+1} f_i^{(k)} \frac{p_{i,A}^T b}{c_i} g_i, \quad k = 1, 2, \dots, n,$$

where the filters

$$(5.7) \quad f_i^{(k)} = 1 - \prod_{j=1}^k \frac{\tilde{c}_j^2 - c_i^2}{\tilde{c}_j^2}, \quad i = 1, 2, \dots, p+1.$$

Proof. Notice that the LSQR algorithm starting with $u_1 = b/\|b\|$ applied to (5.2) is mathematically equivalent to the conjugate gradient (CG) method applied to the normal equation $Q_A^T Q_A w = Q_A^T b$ of (5.2) with the starting vector $w_0 = 0$. Let $w_{ls} = Q_A^\dagger b$ be the solution to $\min_{\tilde{w}} \|Q_A \tilde{w} - b\|$. Then by the SVD (2.2) of Q_A and the notation (5.5) we obtain

$$(5.8) \quad w_{ls} = W_1 P_{1,A}^T b + \sum_{i=2}^{p+1} \frac{p_{i,A}^T b}{c_i} w_i,$$

where the first term is the sum of the $n - p$ SVD components of Q_A corresponding to the largest singular value $c_1 = 1$ with the multiplicity $n - p$.

With our notation and (5.8), keep in mind a well-known result (cf., e.g., [29, Property 2.8]) on the CG iterates that states

$$(5.9) \quad \tilde{w}_k = (I - q_k(Q_A^T Q_A)) w_{ls},$$

where $q_k(\mu)$ is the k -th residual polynomial of CG at iteration k and $q_k(0) = 1$, whose roots are the Ritz values \tilde{c}_j^2 of $Q_A^T Q_A$ with respect to \mathcal{K}_k defined by (5.3), i.e.,

$$q_k(c_i^2) = \prod_{j=1}^k \frac{\tilde{c}_j^2 - c_i^2}{\tilde{c}_j^2}, \quad i = 1, 2, \dots, p+1.$$

Substituting (5.8) into (5.9) yields

$$(5.10) \quad \tilde{w}_k = f_1^{(k)} W_1 P_{1,A}^T b + \sum_{i=2}^{p+1} f_i^{(k)} \frac{p_{i,A}^T b}{c_i} w_i, \quad k = 1, 2, \dots, p+1$$

with $f_i^{(k)}$ defined by (5.7).

Recall from (2.1)–(2.3) that $G = R^{-1}W$. It then follows that $G_1 = R^{-1}W_1$ and $g_i = R^{-1}w_i$, $i = 2, 3, \dots, p+1$. From (5.2), since $x_k = R^{-1}\tilde{w}_k$, premultiplying (5.10) by R^{-1} establishes (5.6) by noticing that $G_1 P_{1,A}^T b = g_\perp$ in our new notation. \square

If $p \geq n$, then $g_\perp = 0$ in (2.8), the first term is zero in (5.6), and the second term becomes

$$x_k = \sum_{i=1}^n f_i^{(k)} \frac{p_{i,A}^T b}{c_i} g_i, \quad k = 1, 2, \dots, n.$$

In this case, (5.6) is a filtered GSVD expansion similar to (2.6). If $p < n$, the first term

$$f_1^{(k)} g_\perp \in \mathcal{N}(L)$$

in (5.6), which resembles the term g_\perp in (2.6) and (2.7). On the other hand,

$$\sum_{i=2}^{p+1} f_i^{(k)} \frac{p_{i,A}^T b}{c_i} g_i$$

in (5.6) corresponds to the first term in (2.6) by noticing that in our notation the indices $i+1$ in the sum correspond to the indices i in (2.6). A difference is that the general-form Tikhonov regularization solution (2.6) and TGSVD solution (2.7) do not affect g_\perp , while our algorithm multiplies it by a factor $f_1^{(k)}$. Nonetheless, $f_1^{(k)} \rightarrow 1$ as \tilde{c}_1 converges to c_1 ; since g_\perp and $f_1^{(k)} g_\perp$ lie in $\mathcal{N}(L)$, they have no effect on Lx_λ , Lx_k^{tgsvd} and Lx_k .

It is known from [10, Theorem 2.1.1, p.23] that the c_i decay like the singular values σ_i of A when the matrix $(A^T, L^T)^T$ is well conditioned, which is true provided that L is well conditioned, as is usually the case in practical applications. In the meantime, notice from (2.2) and (2.3) that Q_A and A share the same P_A and the problems $\min_x \|Ax - b\|$ and $\min_w \|Q_A w - b\|$ have the same right-hand side b . Therefore, the two problems satisfy the same discrete Picard condition.

Furthermore, as has been proved in [15], since the c_i decay and are clustered at zero, the singular values of B_k converge to the large singular values c_i of Q_A in natural order for severely and moderately ill-posed problems until the occurrence of semi-convergence of LSQR for solving $\min_{\tilde{w}} \|Q_A \tilde{w} - b\|$. From (5.6) and (5.7), it is easily justified that $f_i^{(k)} \approx 1$ for $i = 1, 2, \dots, k$ and $f_i^{(k)} \approx 0$ for $i = k+1, \dots, p+1$ when the k Ritz values \tilde{c}_j approximate the large singular values of Q_A in natural order; we refer the reader to [10, pp. 146–148] and [14, 15] for more details. This means that x_k mainly contains the first k dominant GSVD components of $\{A, L\}$ and filters the others corresponding to the small generalized singular values until the semi-convergence of the proposed joint bidiagonalization based method. Precisely, with the equivalence (5.1) and $x_k = R^{-1}\tilde{w}_k$, adapted the results of [15] to our current context, this theorem shows that the proposed joint bidiagonalization based method exhibit typical semi-convergence at some iteration k^* : x_k and Lx_k converge to x_{true} and Lx_{true} for $k \leq k^*$

and afterwards they are deteriorated by the noise e and diverge for $k > k^*$. Therefore, the iteration number k plays the role of the regularization parameter, and the semi-convergence of the joint bidiagonalization based algorithm occurs at iteration k^* , which is such that $\|L(x_{k^*} - x_{true})\|$ is minimal over all $k = 1, 2, \dots, \min\{n, p\}$.

6. The determination of the optimal regularization parameter k^* . For our joint bidiagonalization based algorithm, since the residual norm $\|Ax_k - b\| = \|B_k y_k - \beta_1 e_1\|$ monotonically decreases and the semi-norm $\|Lx_k\| = \|\bar{B}_k y_k\|$ monotonically increases practically with respect to k , the L-curve criterion and the discrepancy principle suit well for a practical determination of k^* . We plot the curve

$$(\log(\|B_k y_k - \beta_1 e_1\|), \log(\|\bar{B}_k y_k\|))$$

and then determine k at its overall corner as an estimate of k^* . This is routine, and we do not repeat the determination procedure; see [10, 11, 12].

If $\|e\|$ or its accurate estimate is known in advance, the discrepancy principle [7, 10, 12] is the simplest and a reliable choice. We stop the algorithm at the first iteration k satisfying

$$(6.1) \quad \|Ax_k - b\| = \|B_k y_k - \beta_1 e_1\| \leq \tau \|e\|$$

with $\tau > 1$ slightly, e.g., $\tau = 1.1$ or smaller. We then use such k as an estimate of the optimal regularization parameter k^* . We mention that a $\tau > 1$ considerably, e.g., $\tau = 2$, is generally unsafe and may underestimate k^* substantially.

Embedded with the above parameter-choice methods, we can now present our joint bidiagonalization based algorithm, called JBDQR and named Algorithm 2.

Algorithm 2 (JBDQR) Given $A \in \mathbb{R}^{m \times n}$ and $L \in \mathbb{R}^{p \times n}$, solve (1.2) and compute the regularized solution x_{k^*} at semi-convergence.

- 1: Starting with $k = 1$, run Algorithm 1, and obtain the small projected problem (4.5).
 - 2: Compute the minimum 2-norm solution y_k to (4.5).
 - 3: Compute $\|Ax_k - b\|$ and $\|Lx_k\|$ by the formulas (4.8) and (4.9).
 - 4: Determine the optimal regularization parameter k^* by the L-curve criterion or check if the discrepancy principle (6.1) is satisfied. If k^* is not found, set $k = k + 1$, and update Algorithm 1. Then go to Step 2.
 - 5: After k^* is determined, form the regularized solution x_{k^*} by solving (4.4).
-

7. Numerical examples. In this section, we report numerical experiments to demonstrate that our JBDQR algorithm works well and the best regularized solutions obtained by it are at least as accurate as those obtained by the hybrid one proposed by Kilmer *et al.* [19] and can be substantially more accurate than the latter ones. We also compare the optimal regularization parameters determined by the L-curve criterion and the discrepancy principle with the true optimal k^* .

We choose some one dimensional examples from the regularization toolbox [11] and some two dimensional problems from the Matlab Image Processing Toolbox and [2, 24]; see Table 1, where the two dimensional image deblurring problems *rice* and *mri* are from the Matlab Image Processing Toolbox. We denote the relative noise level

$$\varepsilon = \frac{\|e\|}{\|b_{true}\|}.$$

For the noise-free problems $Ax_{true} = b_{true}$ in Table 1, we add a white noise e with zero mean and a prescribed noise level ε to b_{true} and form the noisy $b = b_{true} + e$. To simulate exact arithmetic, the complete reorthogonalization is used in Algorithm 1.

TABLE 1
The description of test problems.

Problem	Description	Ill-posedness
shaw	One-dimensional image restoration model [11]	severe
baart	First kind Fredholm integral equation [11]	severe
heat	Inverse heat equation [11]	moderate
deriv2	Computation of second derivative [11]	moderate
rice	Two dimensional image deblurring	unknown
mri	Two dimensional image deblurring	unknown
AtmosphericBlur30	Two dimensional image deblurring [2, 24]	unknown
GaussianBlur422	Two dimensional image deblurring [2, 24]	unknown

We abbreviate Algorithm 2 as JBDQR, the hybrid one in [19] using the GCV and WGCV parameter-choice methods as JBDGCV and JBDWGCV, respectively. Let x_k^{reg} denote the regularized solutions obtained by each of the algorithms. We use the relative error

$$(7.1) \quad \frac{\|L(x_k^{reg} - x_{true})\|}{\|Lx_{true}\|}$$

to plot the convergence curve of each algorithm with respect to k . In the tables to be presented, we will list the smallest relative errors and iteration steps used by JBDGCV and JBDWGCV in parentheses, the optimal iteration steps k^* at which the semi-convergence of JBDQR occurs in the parentheses and the estimated ones for k^* determined by the L-curve criterion and the discrepancy principle (6.1) as well as the corresponding relative errors in the parentheses. We use the Matlab function `lsqr.m` to solve (2.19), (3.5) and (4.4) with the default stopping tolerance $tol = 10^{-6}$.

All the computations are carried out in Matlab R2015b 64-bit on Intel Core i3-2120 CPU 3.30GHz processor and 4 GB RAM with the machine precision $\epsilon_{mach} = 2.22 \times 10^{-16}$ under the Microsoft Windows 7 64-bit system.

7.1. One dimensional case. The test problems *shaw* and *baart* are severely ill-posed, and *heat* and *deriv2* are moderately ill-posed. For each of them we use the code of [11] to generate A , x_{true} and b_{true} . We mention that *deriv2* has three kinds of right-hand sides, distinguished by the parameter "*example* = 1, 2, 3". we only report the results on the parameter "*example* = 2" since we have obtained very similar results on the problem with "*example* = 1, 3". In the experiments, for *shaw* and *baart*, we take $m = n = 1024$, and for ill-posed problems *heat* and *deriv2*, we take $m = n = 3000$; purely for test purposes, we choose

$$(7.2) \quad L = L_1 = \begin{pmatrix} 1 & -1 & & & \\ & 1 & -1 & & \\ & & \ddots & \ddots & \\ & & & 1 & -1 \end{pmatrix} \in \mathbb{R}^{(n-1) \times n},$$

which is a scaled discrete approximation of the first derivative operator in the one dimensional case. We comment that for the scaled discrete approximation of the

second derivative operator, we have observed very similar phenomena. Hence we only report the results on $L = L_1$.

TABLE 2

The relative errors and estimates for the optimal regularization parameters k^ by the L-curve criterion for the test problems with $L = L_1$.*

$\varepsilon = 10^{-2}$				
	JBDGCV	JBDWGCV	JBDQR (k^*)	estimates for k^*
shaw	0.5398(18)	0.5398(18)	0.2094(3)	2(0.2126)
baart	0.5574(7)	0.5574(7)	0.5405(2)	3(0.5625)
heat	0.3758(60)	0.3758(60)	0.2186(13)	5(0.3284)
deriv2	0.4270(60)	0.4270(60)	0.3363(4)	2(0.3853)
$\varepsilon = 10^{-3}$				
	JBDGCV	JBDWGCV	JBDQR (k^*)	estimates for k^*
shaw	0.1930(13)	0.1930(13)	0.1732(5)	2(0.1918)
baart	0.5442(9)	0.5442(9)	0.5038(4)	2(0.5376)
heat	0.1794(100)	0.1794(100)	0.1456(25)	23(0.1485)
deriv2	0.3884(60)	0.3884(60)	0.2635(10)	8(0.3161)
$\varepsilon = 10^{-4}$				
	JBDGCV	JBDWGCV	JBDQR (k^*)	estimates for k^*
shaw	0.1664(14)	0.1664(14)	0.1378(8)	8(0.1378)
baart	0.5346(9)	0.5346(9)	0.4136(5)	3(0.5354)
heat	0.1360(100)	0.1360(100)	0.1275(37)	35(0.1283)
deriv2	0.2916(60)	0.2916(60)	0.2452(15)	12(0.2606)

In Table 2, we display the relative errors of the best regularized solutions by JBDQR, JBDGCV and JBDWGCV with $L = L_1$ and $\varepsilon = 10^{-2}$, 10^{-3} , 10^{-4} , respectively. As we can see from the table, the best regularized solutions by JBDQR are at least as accurate as and can be considerably more accurate than those by JBDGCV and JBDWGCV for all the test problems; see, e.g., **shaw**, **heat** and **deriv2** for $\varepsilon = 10^{-2}$, and **deriv2** for $\varepsilon = 10^{-3}$. We observe from the table that for each test problem the best regularized solution by JBDQR is correspondingly more accurate and requires a bigger k^* for a smaller ε . All these are expected and justify that the smaller ε is, the better regularized solution is extracted, that is, the more GSVD dominant components of $\{A, L\}$ are needed to form it. Finally, for JBDQR, we see that for each problem and given ε , almost all the regularization parameters k^* determined by the L-curve criterion are quite reliable and close to the true k^* except **shaw** for $\varepsilon = 10^{-3}$. But we also find that the the L-curve criterion underestimates the true k^* more or less, that is, the estimates for k^* by the L-curve criterion oversmooths the regularized solutions.

Figure 1 depicts the convergence processes of JBDQR, JBDGCV and JBDWGCV for $L = L_1$ and $\varepsilon = 10^{-3}$. We observe from the figure and Table 2 that, in the most cases, the best regularized solutions by JBDQR are more accurate and can be considerably more accurate than those by JBDGCV and JBDWGCV. In addition, for the severely ill-posed **shaw** and **baart** we find that JBDGCV and JBDWGCV behave very similarly and the convergence processes are almost indistinguishable. Remarkably, we see that the regularized solutions obtained by them converge first, then stabilize for a while, and finally diverge dramatically, while, for **heat** and **deriv2**, they start to stabilize after

TABLE 3

The relative errors and estimates for the optimal regularization parameters k^* by the discrepancy principle for the test problems with $L = L_1$.

$\varepsilon = 10^{-2}$				
	$\tau = 1.005$	$\tau = 1.1$	$\tau = 1.2$	$\tau = 2.0$
shaw	0.3031(1)	0.3031(1)	0.3031(1)	0.3031(1)
baart	0.5421(1)	0.5421(1)	0.5421(1)	0.5421(1)
heat	0.3152(6)	0.3757(3)	0.4629(2)	0.5410(1)
deriv2	0.3853(2)	0.4187(1)	0.4187(1)	0.4187(1)
$\varepsilon = 10^{-3}$				
	$\tau = 1.005$	$\tau = 1.1$	$\tau = 1.2$	$\tau = 2.0$
shaw	0.1888(2)	0.1888(2)	0.1888(2)	0.2338(1)
baart	0.5376(2)	0.5422(1)	0.5422(1)	0.5422(1)
heat	0.1669(20)	0.2196(11)	0.2377(10)	0.3258(5)
deriv2	0.3398(6)	0.4291(2)	0.4291(2)	0.4651(1)
$\varepsilon = 10^{-4}$				
	$\tau = 1.005$	$\tau = 1.1$	$\tau = 1.2$	$\tau = 2.0$
shaw	0.1632(5)	0.1882(3)	0.1882(3)	0.1906(2)
baart	0.5354(3)	0.5354(3)	0.5400(2)	0.5437(1)
heat	0.1356(28)	0.1443(25)	0.1473(24)	0.1745(19)
deriv2	0.2606(12)	0.3019(9)	0.3400(7)	0.3813(4)

k becomes large. We have also observed that the smaller ε is, the later they start to stabilize, though we do not draw all the corresponding figures. The phenomena for **shaw** and **baart** do not comply with the expectation that the regularized solutions ultimately stabilize as the subspace is expanded sufficiently large. The reason is due to the fact that the discrete Picard conditions for the projected problems are satisfied poorly as k increases, as we have argued in the introduction. In contrast, JBDQR has always exhibited the typical semi-convergence for all the problems, which justifies our theory.

Figure 2 depicts the L-curves given by JBDQR with $L = L_1$ and $\varepsilon = 10^{-3}$. We use the function `lcorner` in [11] to determine the overall corner and give an estimate k^* . We see that for the moderately ill-posed problems **heat** and **deriv2** there are much better "L" shape curves, which enable us to determine the optimal k^* more reliably and accurately than those for the severely ill-posed problems **shaw** and **baart**. This is because JBDQR converges very fast and uses very few iterations to achieve the semi-convergence for **shaw** and **baart**. Indeed, the L-curve criterion does not work well for **shaw** and **baart** with $\varepsilon = 10^{-3}$.

Since $\|e\|$ is known for the above test problems, we can use the discrepancy principle (6.1) to estimate the optimal k^* . Table 3 reports the results obtained, in which we have taken the four $\tau = 1.005, 1.1, 1.2$ and 2.0 . Compared with the k^* in Table 2, we have found that the discrepancy principle always underestimate k^* and the problems are over-regularized. We have observed that the reliable determination of k^* critically depend on τ , and the closer τ is to one, the more reliable the estimates are. Particularly, except for **shaw** and **baart** with $\varepsilon = 10^{-2}$, the choice $\tau = 2$ is obviously very bad, and it produces very poor estimates for k^* and leads to considerably less

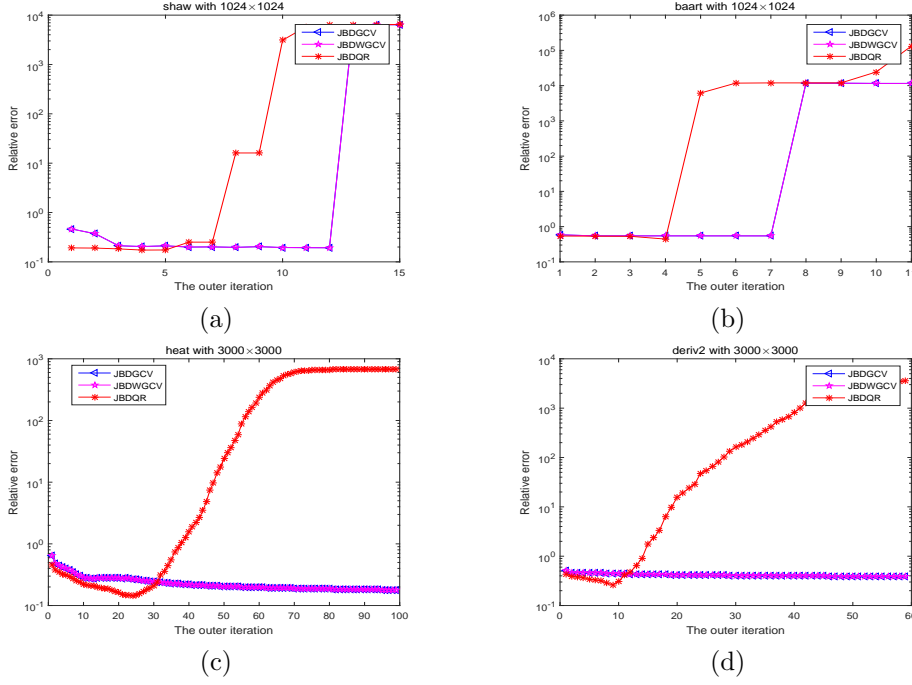


FIG. 1. The relative error of JBDQR, JBDGCV and JBDWGCv with $L = L_1$ and $\varepsilon = 10^{-3}$: (a) shaw; (b) baart; (c) heat; (d) deriv2.

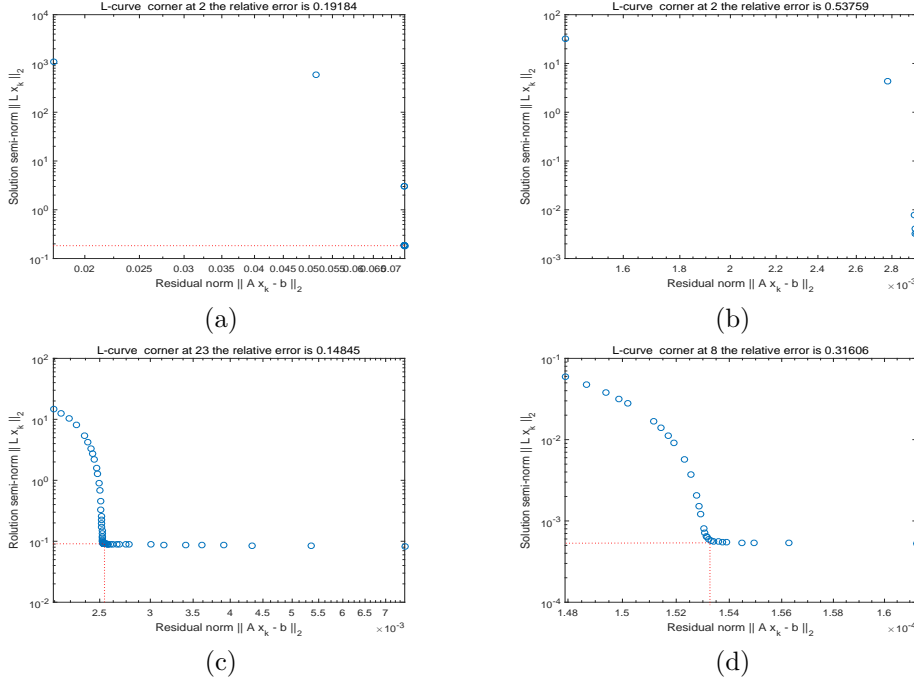


FIG. 2. The determination of k^* by the L-curve criterion by JBDQR with $L = L_1$, $\varepsilon = 10^{-3}$: (a) shaw; (b) baart; (c) heat; (d) deriv2.

accurate regularized solutions than $\tau = 1.005$ does.

7.2. Two dimensional case. In this section, we test some two dimensional image deblurring problems listed in Table 1. The goal is to restore an image x_{true} from a blurred and noisy image $b = b_{true} + e$.

We consider the problems `rice` and `mri` from the Matlab Image Processing Toolbox. The exact image x_{true} of `rice` is an $N \times N$ subimage and that of `mri` is the 15th slice of the three dimensional MRI image dataset which has $N \times N$ pixels. The blurred operator A is a symmetric doubly Toeplitz PSF matrix and is of Kroneck product form $A = (2\pi\sigma^2)^{-1}T \otimes T \in \mathbb{R}^{N^2 \times N^2}$, where $T \in \mathbb{R}^{N \times N}$ is a symmetric banded Toeplitz matrix with half-bandwidth `band` and σ controls the width of Gaussian PSF. In what follows, we use `band` = 16, σ = 2 and N = 128. The size of `rice` and `mri` is $m = n = 128^2 = 16,284$.

We also consider the problems `AtmosphericBlur30` and `GaussianBlur422` of $m = n = 256^2 = 65,536$ from [24]. The blurring of `AtmosphericBlur30` is caused by atmospheric turbulence, and `GaussianBlur422` is spatially invariant Gaussian blur. The exact images are generated by the input command “load `AtmosphericBlur30`” and “load `GaussianBlur422`”, and the blurring operators are generated by the codes `psfMatrix(PSF,center,'zero')` and `psfMatrix(PSF)` from [24], respectively. We abbreviate `AtmosphericBlur30` and `GaussianBlur422` as `blur30` and `blur422`, respectively.

For the experimental purpose, we choose the regularization matrix

$$(7.3) \quad L = \begin{pmatrix} I_N \otimes L_1 \\ L_1 \otimes I_N \end{pmatrix} \in \mathbb{R}^{N(N-1) \times N^2}$$

with L_1 defined in (7.2) and I_N the identity matrix of order N , which is the scaled discrete approximation of the first derivative operator in the two dimensional case incorporating no assumptions on boundary conditions; see [12, Chapter 8.1]. The white noise e with zero mean are generated so that the relative noise levels $\varepsilon = 5 \cdot 10^{-2}$, 10^{-2} and 10^{-3} , respectively.

Besides the smallest relative errors defined by (7.1), Table 4 also lists the relative errors of the corresponding best regularized solutions obtained by JBDGCV, JBDWGCV and JBDQR, which are defined by

$$\frac{\|x_k^{reg} - x_{true}\|}{\|x_{true}\|}$$

and marked “no L ” in the parentheses that follow the matrix names. We can see that for these four problems the solution accuracy of JBDQR is considerably higher than that of JBDGCV and JBDWGCV, no matter which relative error is used. From the table, it is clear that the estimates for k^* by the L-curve criterion are quite rough and considerable underestimates except for `blur30` with $\varepsilon = 10^{-3}$. This indicates that the L-curve criterion does not work well for determining k^* for difficult two dimensional problems. The fundamental cause is that $\|\bar{B}_k y_k\|$ still increases slowly even after $k > k^*$, such that the curve of $(\log(\|B_k y_k - \beta_1 e_1\|), \log(\|\bar{B}_k y_k\|))$ does not form a good L-shape.

Since $\|e\|$ is known for the above test problems, we also use the discrepancy principle criterion (6.1) to estimate the optimal k^* . We report the results obtained when $\tau = 1.005$, 1.1, 1.2 and 2.0 in Table 5. We can see that, for the four $\tau > 1$'s, the regularization parameters determined by the discrepancy principle have big differences for both the solution accuracy and the estimates for k^* . It is obvious that the estimates

TABLE 4
The relative errors and estimates for k^* by the L -curve criterion.

$\varepsilon = 5 \cdot 10^{-2}$				
	JBDGCV	JBDWGCV	JBDQR (k^*)	estimates for k^*
rice	0.8778(3)	0.8736(3)	0.8397(5)	4(0.8411)
rice(no L)	0.1175(3)	0.1142(3)	0.0950(4)	
mri	0.9602(3)	0.9498(4)	0.8848(13)	6(0.9007)
mri(no L)	0.3066(3)	0.2932(3)	0.2324(13)	
blur30	0.9835(3)	0.9827(3)	0.9124(16)	5(0.9521)
blur30(no L)	0.5056(3)	0.4999(3)	0.3036(16)	
blur422	0.9459(9)	0.9443(10)	0.9109(62)	24(0.9203)
blur422(no L)	0.2843(9)	0.2823(10)	0.2522(58)	
$\varepsilon = 10^{-2}$				
	JBDGCV	JBDWGCV	JBDQR (k^*)	estimates for k^*
rice	0.8372(7)	0.8363(7)	0.7774(23)	11(0.7951)
rice(no L)	0.0931(7)	0.0927(7)	0.0764(22)	
mri	0.8923(13)	0.8782(19)	0.8421(51)	25(0.8514)
mri(no L)	0.2367(13)	0.2258(19)	0.2024(50)	
blur30	0.9697(6)	0.9603(9)	0.7975(65)	40(0.8243)
blur30(no L)	0.4238(5)	0.3900(9)	0.2095(65)	
blur422	0.9459(9)	0.9443(10)	0.9109(62)	24(0.9203)
blur422(no L)	0.2843(9)	0.2823(10)	0.2522(58)	
$\varepsilon = 10^{-3}$				
	JBDGCV	JBDWGCV	JBDQR (k^*)	estimates for k^*
rice	0.7638(38)	0.7539(52)	0.7136(166)	145(0.7140)
rice(no L)	0.0726(38)	0.0705(52)	0.0626(163)	
mri	0.8305(101)	0.8225(151)	0.7949(451)	293(0.7988)
mri(no L)	0.1957(101)	0.1917(151)	0.1799(447)	
blur30	0.9628(9)	0.7984(75)	0.5670(433)	577(0.5907)
blur30(no L)	0.3988(9)	0.2060(75)	0.1110(438)	
blur422	0.9137(59)	0.9046(103)	0.8736(542)	284(0.8794)
blur422(no L)	0.2536(59)	0.2471(103)	0.2285(549)	

are much better for $\tau = 1.005$ than those when $\tau = 2$. Again, this indicates that $\tau = 2$ is definitively a very bad choice.

Figure 3 draws the convergence processes of JBDQR, JBDGCV and JBDWGCV for $\varepsilon = 10^{-2}$. We can see that the best regularized solutions by JBDQR are more accurate than the counterparts by JBDGCV and JBDWGCV; the convergence curves of JBDGCV and JBDWGCV first decrease with k , then increase for a while and finally stabilize, but JBDQR has typical semi-convergence phenomenons for all the problems.

A final note on Table 4 and Figure 3 is that the best regularized solutions by JBDWGCV are slightly more accurate than those by JBDGCV, which are different from the previous results in the one dimensional case.

Figure 4 draws the exact images and the reconstructed images for the four test problems with $\varepsilon = 10^{-2}$. Clearly, the reconstructed images by JBDQR are at least as

TABLE 5
The relative errors and estimates for k^* by the discrepancy principle.

$\varepsilon = 5 \cdot 10^{-2}$				
	$\tau = 1.005$	$\tau = 1.1$	$\tau = 1.2$	$\tau = 2.0$
rice	0.8462(3)	0.8556(2)	0.8556(2)	0.8791(1)
mri	0.9007(6)	0.9156(4)	0.9267(3)	0.9653(1)
blur30	0.9181(12)	0.9575(5)	0.9700(3)	0.9849(1)
blur422	0.9444(6)	0.9549(3)	0.9608(2)	0.9707(1)
$\varepsilon = 10^{-2}$				
	$\tau = 1.005$	$\tau = 1.1$	$\tau = 1.2$	$\tau = 2.0$
rice	0.7989(10)	0.8198(6)	0.8267(5)	0.8541(2)
mri	0.8564(21)	0.8652(15)	0.8729(12)	0.8985(6)
blur30	0.8019(56)	0.8285(38)	0.8564(27)	0.9312(9)
blur422	0.9230(21)	0.9308(13)	0.9367(9)	0.9501(4)
$\varepsilon = 10^{-3}$				
	$\tau = 1.005$	$\tau = 1.1$	$\tau = 1.2$	$\tau = 2.0$
rice	0.7288(62)	0.7369(46)	0.7430(38)	0.7709(18)
mri	0.8121(141)	0.8179(105)	0.8223(85)	0.8378(41)
blur30	0.6083(241)	0.6183(216)	0.6286(194)	0.6889(110)
blur422	0.8861(182)	0.8931(119)	0.8972(92)	0.9118(39)

sharp as those by JBDGCV and JBDWGCV, and some of the former ones can be much sharper than the latter, e.g., `blur30`.

For $\varepsilon = 5 \cdot 10^{-2}$ and 10^{-3} , we have similar findings to those in Figures 3–4.

8. Conclusions. In this paper, we have proposed a joint bidiagonalization based algorithm for solving large scale linear discrete ill-posed problems in general-form regularization. This algorithm is different from the hybrid projection based method proposed in [19], which exploits the same joint bidiagonalization process and explicitly regularizes each projected problem generated at every iteration.

We have analyzed the proposed algorithm and established a number of theoretical results. Particularly, we have proved that the iterates take the desired and attractive form of filtered GSVD expansions. The results rigorously show that the algorithm must possess the semi-convergence property and get insight into the regularizing effects of the algorithm. Our algorithm is simpler and easier to implement than the hybrid one, and it is also more reliable and behaves regularly than the latter.

We have made numerical experiments on a number of problems to justify numerous aspects of the proposed algorithm, e.g., solution accuracy and reliability. The results have illustrated that our algorithm often computes considerably more accurate regularized solutions than the hybrid algorithm.

There are some important unsolved problems. As we have seen, a bottleneck of our algorithm and the hybrid one is solve a large scale least squares problem at each outer iteration, which may be costly, especially when the solution accuracy of these problems is high. It is unclear if the solution accuracy can be relaxed substantially, at least at some outer iterations, similar to the randomized SVD algorithms proposed in [17] that solve the general-form regularization problem (1.2). If they could be solved

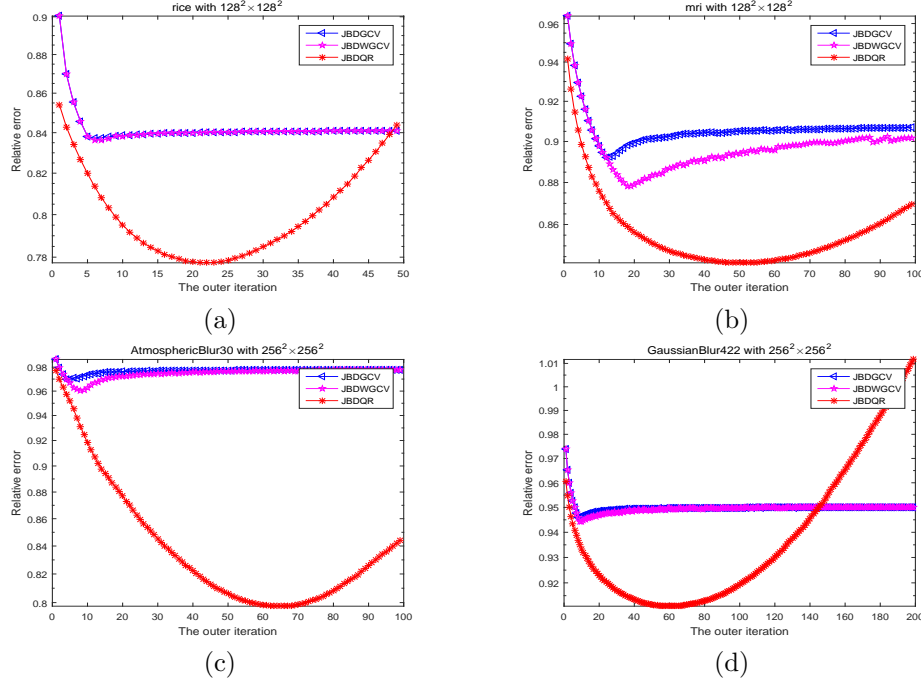


FIG. 3. The relative errors by JBDQR, JBDWGCV and JBDGCV with $\varepsilon = 10^{-2}$: (a) rice; (b) mri; (c) blur30; (d) blur422.

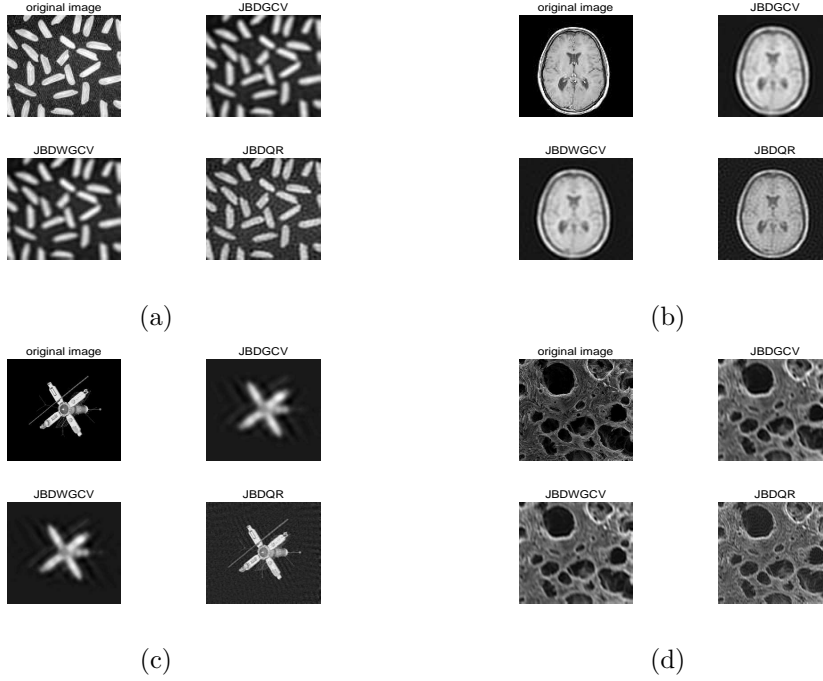


FIG. 4. The exact images and the reconstructed images for the four two dimensional test problems with $\varepsilon = 10^{-2}$: (a) rice; (b) mri; (c) blur30; (d) blur422.

with considerably relaxed accuracy, we shall gain much, and the overall efficiency of the algorithm can be improved substantially. The solution accuracy requirement on the inner least squares problems will constitute our forthcoming work.

REFERENCES

- [1] R. C. ASTER, B. BORCHERS, AND C. H. THURBER, *Parameter Estimation and Inverse Problems*, Second Edition, Elsevier, New York, 2013.
- [2] S. BERISHA AND J. G. NAGY, *Restore Tools: Iterative methods for image restoration*, 2012. Available from <http://www.mathcs.emory.edu/~nagy/RestoreTools>.
- [3] Å. BJÖRCK, *Numerical Methods for Least Squares Problems*, SIAM, Philadelphia, PA, 1996.
- [4] J. CHUNG AND A. K. SAIBABA, *Generalized hybrid iterative methods for large-scale Bayesian inverse problems*, SIAM J. Sci. Comput., 39 (2017), pp. S24–S46.
- [5] J. CHUNG, A. K. SAIBABA, M. BROWN AND E. WESTMAN, *Efficient generalized Golub-Kahan based methods for dynamic inverse problems*, Inverse Probl., 34 (2018), 024005.
- [6] H. W. ENGL, *Regularization methods for the stable solution of inverse problems*, Surveys Math. Indust., 3 (1993), pp. 71–143.
- [7] H. W. ENGL, M. HANKE, AND A. NEUBAUER, *Regularization of Inverse Problems*, Kluwer Academic Publishers, 2000.
- [8] S. GAZZOLA, P. C. HANSEN AND J. G. NAGY, *IR Tools: A Matlab package of iterative regularization methods and large-scale test problems*, arXiv:1712.05602v1 [math.NA], 2017.
- [9] S. GAZZOLA AND P. NOVATI, *Inheritance of the discrete Picard condition in Krylov subspace methods*, BIT Numer. Math., 56 (2016), pp. 893–918.
- [10] P. C. HANSEN, *Rank-Deficient and Discrete Ill-Posed Problems: Numerical Aspects of Linear Inversion*, SIAM, Philadelphia, PA, 1998.
- [11] ———, *Regularization tools version 4.0 for Matlab 7.3*, Numer. Algor., 46 (2007), pp. 189–194.
- [12] ———, *Discrete Inverse Problems: Insight and Algorithms*, SIAM, Philadelphia, PA, 2010.
- [13] M. E. HOCHSTENBACH, L. REICHEL, AND X. YU, *A Golub-Kahan-Type reduction method for matrix pairs*, J. Sci. Comput., 65 (2015) 767–789.
- [14] Z. JIA, *Approximation accuracy of the Krylov subspaces for linear discrete ill-posed problems*, arXiv:math.NA/1805.10132v2, 2018.
- [15] ———, *The low rank approximations and Ritz values in LSQR for linear discrete ill-posed problems*, arXiv:math.NA/1811.03454v1, 2018.
- [16] ———, *The Krylov subspaces, low rank approximations and Ritz values in LSQR for linear discrete ill-posed problems: the multiple singular value case*, (2018), manuscript.
- [17] Z. JIA AND Y. YANG, *Modified truncated randomized singular value decomposition (MTRSVD) algorithms for large scale discrete ill-posed problems with general-form regularization*, Inverse Probl., 34 (2018), 055031.
- [18] J. KAIPIO AND E. SOMERSALO, *Statistical and Computational Inverse Problems*, Applied Mathematical Sciences 160, Springer, 2005.
- [19] M. E. KILMER, P. C. HANSEN, AND M. I. ESPANOL, *A projection-based approach to general-form Tikhonov regularization*, SIAM J. Sci. Comput., 29 (2007), pp. 315–330.
- [20] M. E. KILMER AND D. P. O’LEARY, *Choosing regularization parameters in iterative methods for ill-posed problems*, SIAM J. Matrix Anal. Appl., 22 (2001), pp. 1204–1221.
- [21] R. LI AND Q. YE, *A Krylov subspace method for quadratic matrix polynomial with application to constrained least squares problems*, SIAM J. Math. Anal., 25 (2003), pp. 405–428.
- [22] K. MILLER, *Least squares methods for ill-posed problems with a prescribed bound*, SIAM J. Math. Anal., 1 (1970), pp. 52–74.
- [23] E. NATTERER, *The Mathematics of Computerized Tomography*, John Wiley, New York, 1986.
- [24] J. G. NAGY, K. PALMER, AND L. PERRONE, *Iterative methods for image deblurring: A Matlab object-oriented approach*, Numer. Algor., 36 (2004), pp. 73–93.
- [25] C. C. PAIGE AND M. A. SAUNDERS, *LSQR: An algorithm for sparse linear equations and sparse least squares*, ACM Trans. Maths. Soft., 8 (1982), pp. 43–71.
- [26] B. N. PARLETT, *The Symmetric Eigenvalue Problem*, SIAM, Philadelphia, PA, 1998.
- [27] R. A. RENAUT, S. VATANKHAH, AND V. E. ARDESTA, *Hybrid and iteratively reweighted regularization by unbiased predictive risk and weighted GCV for projected systems*, SIAM J. Sci. Comput., 39 (2017), pp. B221–B243.
- [28] L. REICHEL, F. SGALLARI, AND Q. YE, *Tikhonov regularization based on generalized Krylov subspace methods*, Appl. Numer. math., 62 (2012), pp. 1215–1228.
- [29] A. VAN DER SLUIS AND H. A. VAN DER VORST, *The rate of convergence of conjugate gradients*, Numer. Math., 48 (1986), pp. 543–360.

- [30] I. N. ZWAAN AND M. HOCHSTENBACH, *Multidirectional subspace expansion for one-parameter and multiparameter Tikhonov regularization*, J. Sci. Comput., 70 (2017), pp. 990–1007.
- [31] H. ZHA, *Computing the generalized singular values/vectors of large sparse or structured matrix pairs*, Numer. Math., 72 (1996), pp. 391–417.